Sixth International Symposium on Turbulence and Shear Flow Phenomena
Seoul, Korea, 22-24 June 2009

ZONAL FLOWS IN MAGNETOHYDRODYNAMIC (MHD) TURBULENCE

Salah Neffaa
M2P2-CNRS, Université de Provence,
39 rue Joliot-Curie, 13453 Marseille Cedex 13, France,
neffaa@L3m.univ-mrs.fr

Wouter J. T. Bos
LMFA, UMR CNRS 5509, Ecole Centrale de Lyon - Université Claude Bernard Lyon 1 - INSA de Lyon,
69134 Ecully Cedex, France,
wouter.bos@ec-lyon.fr

Kai Schneider
M2P2-CNRS & CMI, Université de Provence,
39 rue Joliot-Curie, 13453 Marseille Cedex 13, France,
kschneid@cmi.univ-mrs.fr

ABSTRACT

Spontaneous spin-up of two-dimensional MHD turbulence is investigated in different wall-bounded geometries by means of direct numerical simulation. It is shown that in square and elliptic geometries the flow has a strong tendency to generate angular momentum from initial conditions free from angular momentum. In circular geometry this tendency is absent. It is shown that the generation of angular momentum in non-axisymmetric geometries can be enhanced by increasing the magnetic pressure. The effect is stronger at higher Reynolds numbers. The generation of angular fields, (or magnetic angular momentum), previously observed at low Reynolds numbers, is weak but persistent in both the circular and elliptic geometries.

INTRODUCTION

In fusion plasmas, spontaneous large-scale poloidal rotation is beneficial for the confinement as it suppresses turbulence and radially extended structures, which are largely responsible for anomalous transport [2, 11]. This reduction of turbulent activity plays a key role in the transition to an improved confinement state (L-H transition) [5]. The absence of this transition would jeopardize the success of the ITER project. The understanding of large scale poloidal rotation is therefore primordial. It is generally admitted that the poloidal rotation of tokamaks is due to the asymmetry of the charge distribution. However, in recent work [12] the link was made between the L-H transition and the inverse cascade of two-dimensional turbulence. A neutral fluid can therefore also give rise to poloidal large-scale rotation.

The phenomenon of spontaneous generation of large-scale rotation-cells in two-dimensional fluid turbulence was discovered by Clercx *et al.* [4]. The importance of the non-axisymmetry of the geometry was recently demonstrated by Keetels *et al.* [6], and an interpretation in terms of statistical mechanics was obtained by Taylor *et al.* [13]. All these studies were performed for non–conducting fluids, using either the Navier–Stokes, or Euler equations. In MHD turbulence the question was investigated for the first time only very recently [3], where it was shown that spin-up in MHD turbulence is also present and that it can be enhanced by increasing the magnetic fluctuations. These observations were however done at low Reynolds numbers in square and circular geometries. In the present work we will confirm these results at higher Reynolds numbers in three different geometries, a square, a circle and an ellipse. It is shown that the tendency to generate angular momentum is stronger at higher Reynolds number. The tendency to generate angular fields is still present at these Reynolds numbers, but not in the square geometry.

METHOD

We present results of pseudo-spectral simulations of two-dimensional MHD turbulence in bounded domains. An efficient method to compute these flows is the penalization method, which was introduced by Angot *et al.* [1], and applied to fluid turbulence by Schneider [9, 10]. This method was extended to MHD turbulence in a recent work [8]. Using this method, efficient pseudo-spectral solvers can be used to compute flows which contain solid walls and obstacles.

The simulations are performed in circular, square and elliptic domains. No-slip boundary conditions are imposed for the velocity field and the normal component of the magnetic field vanishes at the wall, while the tangential component freely evolves. The governing equations are

$$\frac{\partial \boldsymbol{u}}{\partial t} + \boldsymbol{u}\cdot\nabla\boldsymbol{u} = -\nabla p + \boldsymbol{j}\times\boldsymbol{B} + \nu\nabla^2\boldsymbol{u} - \frac{1}{\epsilon}\chi(\boldsymbol{u}-\boldsymbol{u_0}) \quad (1)$$

$$\frac{\partial \boldsymbol{B}}{\partial t} = \nabla\times(\boldsymbol{u}\times\boldsymbol{B}) + \eta\nabla^2\boldsymbol{B} - \frac{1}{\epsilon}\chi(\boldsymbol{B}-\boldsymbol{B_0}) \quad (2)$$

$$\nabla\cdot\boldsymbol{u} = 0 \quad (3)$$

$$\nabla\cdot\boldsymbol{B} = 0 \quad (4)$$

Here ν and η are respectively the kinematic viscosity and the magnetic diffusivity. The vorticity is defined by $\omega\mathbf{e_z} = \nabla\times\mathbf{u}$ and $j\mathbf{e_z} = \nabla\times\mathbf{B}$ denotes the current density. Furthermore we define the vector potential $\mathbf{a} = \mathrm{a}\mathbf{e_z}$ as $\mathbf{B} = \nabla\times\mathbf{a}$ and the stream function ψ as $\mathbf{u} = \nabla^{\perp}\psi = (-\partial\psi/\partial y, \partial\psi/\partial x)$. The last term in the evolution equations for $\boldsymbol{u}$ and $\boldsymbol{B}$, is the penalization term which allows to impose the solid boundary conditions.

The quantities $\mathbf{u_0}$ and $\mathbf{B_0}$ correspond to the values imposed in the solid part of the numerical domain. Here we choose $\mathbf{u_0} = \mathbf{0}$ and $\mathbf{B_0} = \mathbf{B}_\parallel$ (where $\mathbf{B}_\parallel$ is the tangential component of $\mathbf{B}$ at the wall), corresponding to vanishing velocity and no penetration of magnetic field into the solid domain which is hence considered as a perfect conductor, see also [7]. In other terms there is no magnetic flux across the wall. The mask function χ is equal to 0 inside the fluid domain (where the penalization terms thereby dissappear) and equal to 1 inside the part of the domain which is considered to be a solid. The physical idea is to model the solid part as a porous medium whose permeability ϵ tends to zero [1, 9]. For $\epsilon \to 0$, where the obstacle is present, the velocity $\mathbf{u}$ tends to $\mathbf{u_0}$ and the magnetic field $\mathbf{B}$ tends to $\mathbf{B_0}$. The nature of the boundary condition for the velocity is thus no-slip at the wall.

The initial conditions consist of correlated noise, with a prescribed energy spectrum, peaked at the low wavenumbers. The initial fields contain zero or little angular momentum and angular field, defined respectively as

$$\begin{aligned} L_u &= \int_\Omega \boldsymbol{e}_z \cdot (\boldsymbol{r} \times \boldsymbol{u})\, dA, \\ L_B &= \int_\Omega \boldsymbol{e}_z \cdot (\boldsymbol{r} \times \boldsymbol{B})\, dA. \end{aligned} \tag{5}$$

in which Ω is the flow domain and r is the position vector with respect to the center of the domain. Simulations are performed at a resolution of 512^2 grid-points. The magnetic Prandtl number is unity and the initial Reynolds number, based on the root mean square velocity, and domain-size is of the order of 10^4. Ten simulations were carried out in each geometry and we present the results of the simulations in which the generation of angular momentum is maximal. The time is normalized by $D/\sqrt{2E_u(t=0)}$, D being the typical lengthscale of the fluid domain.

RESULTS

Visualizations

Visualizations of the vorticity, the stream-function the current density and the vector-potential are displayed in Figure 1. We will first focus on the behavior in the square geometry. It is observed that both in the velocity-field and the magnetic field exhibit a tendency to generate large-scale structures. The current-density shows that the magnetic field-lines of the two main flow-structures are in the opposite direction. This is even clearer in the plot of the vector potential. The magnetic angular momentum L_B is therefore small, since the contributions of both structures cancel each other out. For the velocity field this is not the case. Significant symmetry-breaking is observed, especially in the stream-function. Both vortices are turning in the same sense, with a strong shearing region in between them. Non-zero angular momentum results. Similar observations can be made for the elliptic geometry. In the circular geometry it is more difficult to visually evaluate the generation of angular momentum.

Quantifying the generation of kinetic and magnetic angular momentum

To quantify the extend to which a large-scale swirling structure dominates the flow, we plot in Figure 2 the angular momentum in the three geometries. It is observed that strong spin-up takes place in the square and in the ellipse. The generation of the angular momentum is spontaneous, after a short time interval $t \approx 3$ and one observes that the amplitude is close to 0.4 in the square and 0.3 in the ellipse. This implies that, in the square container, the fluid reaches an angular momentum which corresponds to approximately 40% of the angular momentum which would possess a fluid in solid-body rotation containing the same energy at $t = 0$. There is practically no spin-up in the circular container.

In Figure 2, bottom, the magnetic angular momentum is evaluated in all geometries. Surprisingly, in the square in which the generation of kinetic angular momentum was the strongest, L_B remains close to zero. In the other two geometries, an amount of L_B is created, however, this magnetic spin-up takes place on a time-scale which is larger than for its kinetic counterpart. Furthermore it can be observed that once L_B is created it remains almost constant over time.

Discussion

In [3] we derived the equation for L_u in the case of MHD turbulence. It reads

$$\frac{dL_u}{dt} = \nu \oint_{\partial\Omega} \omega(\boldsymbol{r} \cdot \boldsymbol{n}) ds + \oint_{\partial\Omega} p^\star \boldsymbol{r} \cdot d\boldsymbol{s} \tag{6}$$

with ν the kinematic viscosity, ω the vorticity, $\boldsymbol{n}$ the unit-vector perpendicular to the wall, $p^\star = p + B^2/2$ is the sum of the hydrodynamic and magnetic pressure. It was discovered by Clercx et al. [4] that spontaneous generation of angular momentum in hydrodynamic turbulence is observed in square domains, whereas it is absent in a circular domain. Subsequently, it was explained to be an effect due to the pressure [6], the last term in equation (6). Indeed, this term vanishes in a circular domain. In MHD, the presence of the magnetic pressure allows to vary the importance of the pressure term, while keeping the other parameters constant, by changing the value of the magnetic fluctuations. This is illustrated in Figure 3. The ratio E_B/Eu is varied, with E_B the mean-square of the magnetic fluctuations and E_u the mean-square of the velocity fluctuations. It is observed that the tendency to spin-up is significantly increased in the square geometry. It is thus shown that both geometry and magnetic pressure can play a role in the generation of zonal flows.

In [3], the tendency to generate angular fields was also investigated by computing the value of L_B. It was observed that angular fields were observed, even in the circular geometry. In Figure 2 bottom, we show that at higher Reynolds numbers the generation of this 'magnetic angular momentum' is weak but persistent. In the square geometry it is absent. Writing the equation for L_B, we find

$$\frac{dL_B}{dt} = \eta \oint_{\partial\Omega} j(\boldsymbol{r} \cdot \boldsymbol{n}) ds - 2\eta I\,. \tag{7}$$

where I denotes the net current through the domain, defined by $I = \int_\Omega j dA$. The pressure plays thus no direct role and only the net current or resistive magnetic stress can generate angular fields. It is surprising that in the circular geometry the generation of angular fields is present, whereas it is absent in the square geometry. We suspect that it is related to the presence of a mean current through the circular domain. However, for the moment the reason for this is not understood and thus requires further investigations.

CONCLUSIONS

Pseudo-spectral simulations of two-dimensional MHD turbulence in a bounded domain were performed. It was shown that spin-up takes place in non-axi-symmetric geometries (squares, ellipses). This phenomenon, observed in [3] at

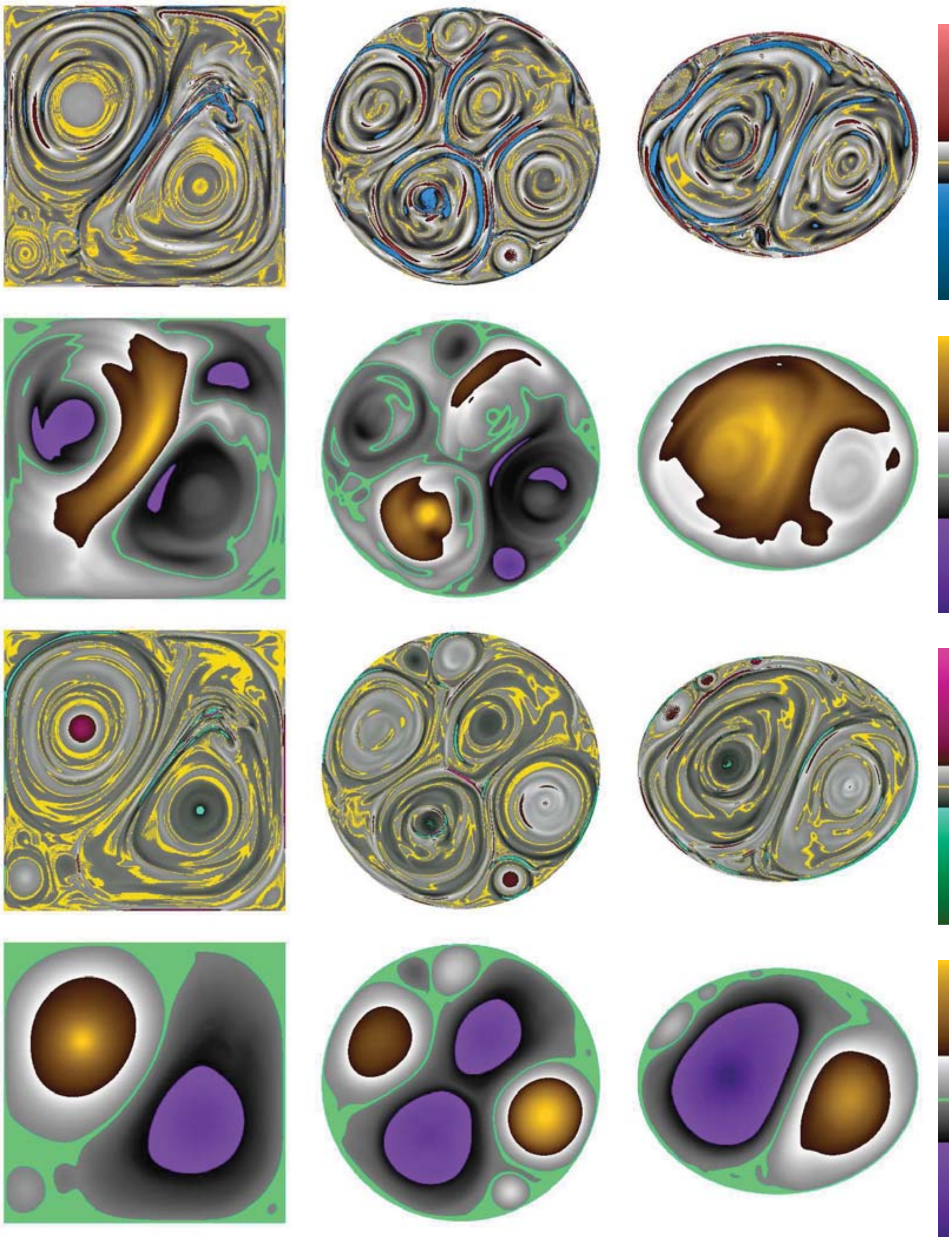

Figure 1: Visualizations of (from top to bottom) the vorticity ω, the stream–function ψ, the current density j and the vector potential a for the square, circular and elliptic geometries. The three columns correspond to (from left to right) to the time instants $t^{\star} = 3, 2, 2.7$ for which L_u (Fig. 2) is maximal. The time is normalized by the initial turn-over time.

low Reynolds number, persists at higher Reynolds numbers (larger by about a factor 6) and becomes more pronounced. The generation of the magnetic equivalent of the angular momentum becomes weaker at higher Reynolds numbers. The first effect, the kinetic spin-up can be enhanced by increasing the magnetic fluctuations. It is therefore clearly related to the pressure term p^{*}. The fact that the magnetic spin-up is persistent at these Reynolds numbers might be related to the presence of a net current through the domain.

ACKNOWLEDGMENTS

We thankfully acknowledge financial support from the ANR, project M2TFP and KS also thanks the Institut Carnot STAR for partial financial support.

References

[1] P. Angot, C.H. Bruneau, and P. Fabrie. A penalization method to take into account obstacles in viscous flows. *Numer. Math.*, 81:497, 1999.

[2] H. Biglari, P.H. Diamond, and P.W. Terry. Influence of sheared poloidal rotation on edge turbulence. *Phys. Fluids B*, 2:1, 1990.

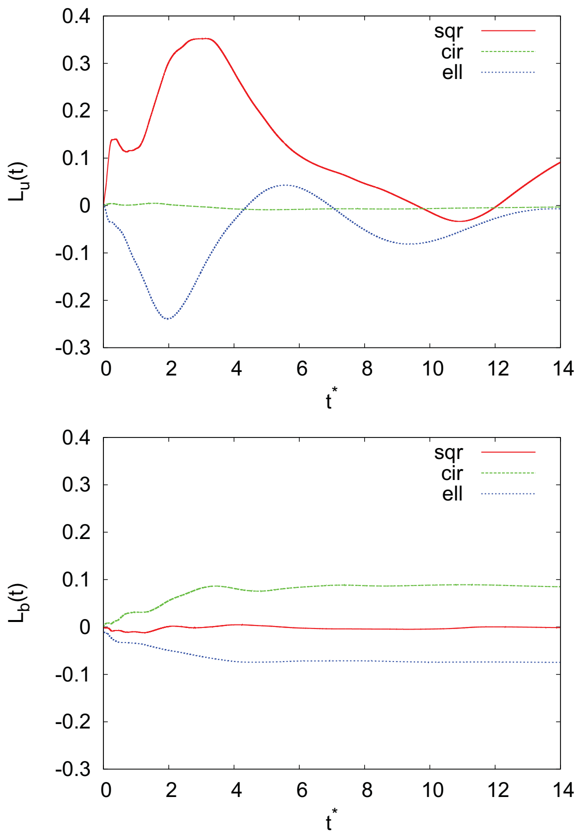

Figure 2: Time-dependence of the angular momentum L_u (top) and angular field L_B (bottom) in the square, circular and elliptic geometry, normalized by $\mathcal{L}_u(0)$ and $\mathcal{L}_B(0)$, respectively.

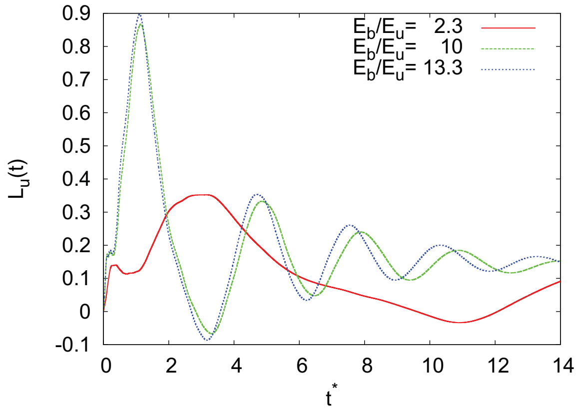

Figure 3: The influence of the magnetic pressure on the spin-up in the square container is illustrated by changing the ratio E_B/E_u, while keeping E_u fixed.

[3] W.J.T. Bos, S. Neffaa, and K. Schneider. Rapid generation of angular momentum in bounded magnetized plasma. *Phys. Rev. Lett.*, 101:235003, 2008.

[4] H. J. H. Clercx, S.R. Maassen, and G.J.F.van Heijst. Spontaneous spin-up during the decay of 2d turbulence in a square container with rigid boundaries. *Phys. Rev. Lett.*, 80:5129, 1998.

[5] F. Wagner *et al.* Regime of improved confinement and high beta in neutral-beam-heated divertor discharges of the ASDEX tokamak. *Phys. Rev. Lett.*, 49:1408, 1982.

[6] G.H. Keetels, H.J.H. Clercx, and G.J.F. van Heijst. Spontaneous angular momentum generation of 2d flows in an elliptical geometry. *Phys. Rev. E*, 78:036301, 2008.

[7] P.D. Mininni and D.C. Montgomery. Magnetohydrodynamic activity inside a sphere. *Physics of Fluids*, 18:116602, 2006.

[8] S. Neffaa, W.J.T. Bos, and K. Schneider. The decay of magnetohydrodynamic turbulence in a confined domain. *Phys. Plasmas*, 15:092304, 2008.

[9] K. Schneider. Numerical simulation of the transient flow behaviour in chemical reactors using a penalization method. *Comput. Fluids*, 34:1223, 2005.

[10] K. Schneider and M. Farge. Decaying two-dimensional turbulence in a circular container. *Phys. Rev. Lett.*, 95:244502, 2005.

[11] X. Shan and D.C. Montgomery. Magnetohydrodynamic stabilization through rotation. *Phys. Rev. Lett.*, 73:1624, 1994.

[12] M. G. Shats, H. Xia, and H. Punzmann. Spectral condensation of turbulence in plasmas and fluids and its role in low-to-high phase transitions in toroidal plasma. *Phys. Rev. E*, 71:046409, 2005.

[13] J.B. Taylor, M. Borchardt, and P. Helander. Interacting vortices and spin-up in two-dimensional turbulence. *Phys. Rev. Lett.*, 102:124505, 2009.